PERK-mediated induction of miR-5p and miR-3p arms of miR-616 regulates cell growth by targeting c-MYC

Afrin Sultana[1†], Ananya Gupta[2] and Sanjeev Gupta[1*]

[1] Discipline of Pathology, School of Medicine, Clinical Science Institute, Lambe Institute for Translational Research, University of Galway, Galway, Ireland

[2] Discipline of Physiology, School of Medicine, University of Galway, Galway, Ireland

*Corresponding author
Email: sanjeev.gupta@universityofgalway.ie

Keywords: unfolded protein response, ER stress, miR-616, c-MYC, breast cancer

ABSTRACT

C/EBP homologous protein (CHOP), also known as DNA damage-inducible transcript 3 (DDIT3), is a member of CCAAT/enhancer-binding protein (C/EBP) family. The expression of CHOP is upregulated during unfolded protein response (UPR), and sustained CHOP activity plays an important role in UPR-induced apoptosis. MicroRNA-616 is localized in an intron of the CHOP gene. However, regulation of miR-616 expression during UPR and its function in breast cancer is not clearly understood. We show that miR-5p/-3p arms of miR-616 are expressed with levels of 5p arm higher than 3p arm. During conditions of UPR, the expression of miR-5p and miR-3p arms of miR-616 and its host gene (CHOP) was concordantly increased primarily in a PERK-dependent manner. We show that ectopic expression of miR-616 significantly suppressed cell growth and colony formation, whereas knockout of miR-616 increased it. We identified that MYC proto-oncogene (c-MYC) gene is repressed during the UPR and targeted by miR-616. Further, we show that expression of miR-616 and CHOP is downregulated in human breast cancer, where expression of miR-616 was associated with poor overall survival (OS) in luminal A subtype and better OS HER2 subtype of breast cancer. In summary, our results suggest a dual function for the DDIT3 locus, where CHOP protein and miR-616 can co-operate to regulate cancer progression.

56 # INTRODUCTION

57 The endoplasmic reticulum (ER) is a crucial cellular organelle that plays important role in
58 folding and maturation of proteins that transit through the secretory pathway. Stimuli that
59 compromise the protein handling capacity of the ER activate an evolutionarily conserved
60 pathway known as unfolded protein response (UPR). Three major sensor molecules that
61 initiate the UPR are activating transcription factor 6 (ATF6), inositol-requiring enzyme 1α
62 (IRE1) and protein kinase RNA-like endoplasmic reticulum kinase (PERK) (1). During resting
63 state the activity of PERK, IRE1 and ATF6 is kept under control by interaction with ER
64 chaperone glucose-regulated protein 78 (GRP78); however, upon accumulation of misfolded
65 proteins in ER, GRP78 dissociates from these molecules, leading to their activation (2). Upon
66 dissociation with GRP78, IRE1 auto-phosphorylates and oligomerizes leading to the activation
67 of its endoribonuclease domain present in the cytosolic domain. Active IRE1 catalyses the
68 unconventional splicing of XBP1 mRNA and regulated IRE1-dependent decay of transcripts
69 (RIDD) (3). While splicing of XBP1 mRNA is an adaptive response to UPR, RIDD has many
70 context dependent outcomes (3). ATF6 is a transmembrane protein located in the ER
71 membrane with an N-terminus cytoplasmic domain containing a DNA-binding motif and a C-
72 terminus ER-luminal domain that interacts with GRP78 (4). During UPR, ATF6 is relocates from
73 the ER to the Golgi compartment. In the Golgi, ATF6 is processed by intramembranous
74 proteolysis causing the release of the transcriptionally active N-terminal cytosolic domain,
75 p50ATF6 (5). During UPR, active PERK phosphorylates eukaryotic initiation factor 2α (eIF2α),
76 causing reduced translation initiation for a majority of cellular proteins and preferential
77 translation of a subset of mRNAs including activating transcription factor 4 (ATF4) (6, 7).
78 Phosphorylation of eIF2α leads to general translational block and preferential translation of

79 a subset of mRNAs including activating transcription factor 4 (ATF4) (7). Phosphorylation of
80 NRF2 by PERK attenuates Keap1-mediated degradation of NRF2 and promotes expression of
81 NRF2-target genes through the antioxidant response elements (ARE) (6). The increased
82 protein handling capacity of the ER and degradation of unfolded proteins induced by UPR
83 attempts to restore the protein homeostasis and increase cell survival. However, if UPR-
84 induced mechanisms fail to alleviate ER stress, UPR activates apoptosis.
85
86 MicroRNAs (miRNAs) are small (~20–23 nucleotide) single-stranded RNA molecules that
87 regulate gene expression in a sequence-specific manner (8). The increased expression of miR-
88 616 has been reported in androgen-independent prostate cancer (9, 10), gastric cancer (11),
89 non-small cell lung cancer (NSCLC) (12), hepatocellular carcinoma (HCC) (13) and gliomas
90 (14). MiR-616 targets tissue factor pathway inhibitor (TFPI-2) in prostate cancer (9); PTEN in
91 HCC and gastric cancer (15); SOX7 in glioma and NSCLC (14). However, miR-616-3p has been
92 reported to reduce XIAP expression and potentiate apoptosis in HUVECs (16). LINC01614
93 promotes head and neck squamous cell carcinoma progression via PI3K/AKT signalling
94 pathway and miR-616-3p can inhibit cancer progression by downregulating LINC01614
95 expression (17). Ye et al. reported that miR-616-3p inhibited cell growth and mammosphere
96 formation of breast cancer cells by suppressing GLI1 (18), while Yuan reported that miR-616-
97 3p promoted breast cancer cell migration and invasion by targeting TIMP2 and regulating
98 MMP signalling (19). Overall, these observations suggest that miR-616 exhibits both
99 oncogenic and tumour suppressor functions in context- and/or tissue-dependent manner.
100 Additional studies are warranted to further investigate the role of miR-616 in human cancers.
101

102 During the past few years, work from several groups has revealed that all three branches of
103 the UPR regulate specific subsets of miRNAs (20, 21, 22, 23). The modes of regulation include
104 both increase and decrease in expression by UPR-regulated transcription factors such as ATF6,
105 XBP1, ATF4 and NRF2 as well as degradation by RIDD activity. The key feature of UPR-
106 dependent miRNA expression is fine tuning of the ER homeostasis to modulate cellular
107 adaptation to stress and regulation of cell fate. The gene encoding miRNA-616 is located in
108 the second intron of CHOP/DDIT3. This genomic co-location of miR-616 with CHOP/DDIT3
109 suggests a role for miR-616 in UPR. Indeed, increased expression of miR-616 has been
110 reported during conditions of UPR (24, 25). Hiramatsu et al., focused on the expression of
111 miR-616-5p (24) while Arabkari focused on the expression of miR-616-3p (25). Here we have
112 evaluated the expression of both miR-5p/-3p arms of miR-616 as well its host gene (CHOP)
113 during conditions of UPR.
114
115 We show that expression level of miR-616-5p was higher than miR-616-3p in human cancer
116 cells and tissues. During conditions of UPR, the expression of both miR-5p/-3p arms of miR-
117 616 and CHOP was increased in a PERK-dependent manner. Our results show that miR-616
118 regulates cell growth and proliferation along with regulation of c-MYC expression. We
119 identified that MYC proto-oncogene (MYC) gene is repressed during the UPR and targeted by
120 miR-616. Finally, we show that expression of miR-616 and CHOP (host gene of miR-616) is
121 reduced in human breast cancer. The. In summary, our results suggest that CHOP locus
122 generates two gene products, where CHOP protein and miR-616 can act together to regulate
123 cancer progression.
124
125 **METHODS**

126 **Cell culture and treatments** - Human breast cancer cells (MCF7 and BT474) were purchased
127 from ECACC. HCT116 cells were kind gift from Dr. Victor E. Velculescu, Johns Hopkins
128 University, USA. HEK 293T cells were gift from Indiana University National Gene Vector
129 Biorepository. The MCF7, BT474 and HEK 293T cells were maintained in Dulbecco's modified
130 eagle's medium. HCT116 cells were maintained in McCoy's 5A modified. The medium was
131 supplemented with 10% heat inactivated foetal bovine serum (FBS) and 100 U/ml penicillin
132 and 100 µg/ml streptomycin with 5% CO2 at 37°C. Thapsigargin (Cat # 1138) and BFA (Cat #
133 1231) were purchased from Tocris Bioscience. All reagents were purchased from Sigma-
134 Aldrich unless otherwise stated.
135
136 **Plasmid constructs** - miExpressTM precursor miRNA expression clones, miR-CTRL and miR-
137 616 (pEZX-MR03 vector) were sourced from GeneCopoeia, Rockville, MD, USA. The lentiviral
138 plasmids pLV [CRISPR]-hCas9:T2A: Puro-U6>mir-616 expressing hCas9 protein and miR-616
139 targeting gRNA were obtained from VectorBuilder Inc, Chicago, IL, USA. The sequences of
140 two miR-616 targeting gRNAs are 5'-GGAAATAGGAAGTCATTGGA-3' and 5'-
141 GTGTCATGGAAGTCACTGAA-3'. PCDH-Flag-c-MYC was a gift from Hening Lin (Addgene
142 plasmid # 102626; http://n2t.net/addgene:102626; RRID: Addgene_102626).
143
144 **Generation of stable cell lines** – MCF7 cells were transduced with lentiviruses to generate
145 stable miR-616 overexpressing and miR-616 knockout sub-clones. Lentivirus was generated
146 by transfecting lentiviral plasmids along with packaging plasmids in 293T cells using jetPEI
147 transfection reagent as described previously (26).
148

149 **RNA extraction, Reverse transcription reaction and real time quantitative PCR** - Total RNA
150 was isolated using Trizol (Life Technologies) according to the manufacturer's instructions.
151 RPLP0 and GAPDH (for mRNAs) and U6 SnRNA (for miRNAs) were used as a reference genes
152 to determine the relative expression level of target genes between treated and control
153 samples using △△Ct method.
154
155 **Colony formation assay** - The cells were plated in 6 well plates and were grown for 14 days.
156 After 14 days, cells were washed twice with PBS and fixed with 10% formaldehyde for 5
157 minutes and stained with 0.5 % crystal violet for 10 minutes. The number of colonies were
158 counted in five random view fields under a microscope and average number of colonies was
159 determined. Colony size was determined using Image J software.
160
161 **X-CELLigence cell proliferation assay** - xCELLigence experiments were performed using the
162 Real-Time Cell Analyzer (RTCA) Dual Plate (DP) instrument according to the manufacturer's
163 instructions (Agilent.com). Briefly, instrument-specific specially designed gold
164 microelectrodes fused microtiter 16-well cell culture plate (0.2 cm2 well surface area; 250 µl
165 volume per well) was used to monitor the real-time changes expressed as Cell index (CI).
166 Cell Index is defined as (Rn−Rb)/15 where Rn is the cell–electrode impedance of the well
167 with the cells and Rb is the background impedance of the well with the medium alone. The
168 background impedance was measured by adding 50 µl of medium to each well of the E-Plate
169 before seeding the cells. After seeding (2500 cells/well), the E-plate was incubated at room
170 temperature for 30 min and then transferred to the instrument. Cell proliferation was
171 monitored every 15 min for 50 h.
172

173 **Western blot analysis** - Western blotting procedure has been described previously. After
174 blocking with specific solution nitrocellulose membranes were treated with specific primary
175 antibodies including c-MYC (Santa Cruz Biotechnology Cat# sc-40), ERα (Merck Millipore
176 Cat# 2828587) and β-Actin (Sigma, Cat# A-5060) at 4°C for overnight. After washing three
177 times with PBS/0.05%Tween solution, the membranes were incubated with appropriate
178 secondary antibody at room temperature for 2 hours. The membranes were then washed
179 twice with PBS/0.05%Tween and once with PBS and finally the signals were detected using
180 Western Lightening chemiluminescent substrate (Perkin Elmer, Netherlands, Cat
181 #NEL104001EA).
182
183 **Statistical Analysis** - The GraphPad was used for statistical analysis and generating graphs.
184 Two-tailed unpaired t-test was performed to determine statistically significant differences
185 between independent groups. Results with a $p<0.05$ were considered statistically significant.
186

187 # Results

188 ## Expression of miR-616-5p is higher than miR-616-3p

189 Several miRNAs are located within the introns of either protein coding or non-coding genes,
190 and are referred to as intronic miRNAs (27). The genes which harbour these miRNAs are
191 embedded are called host genes. MiR-616 is an intronic miRNA localized in the first intron of
192 DDIT3 gene (**Fig 1A**). Both the 5' and 3' arms of the precursor duplex can generate mature
193 miRNAs, and are referred to as miRNA-5p and -3p (27, 28). The miRBase
194 (http://www.mirbase.org) (29) has discontinued the use of miRNA/miRNA* nomenclature
195 and use of miR-5p and miR-3p nomenclature (30), based solely on 5'- or 3'-arm derivation of

196 the mature miRNA is now recommended. The sequences of mature miR-616, accession
197 numbers and the previous names of miR-616-5p and -3p as per miRNA/miRNA* nomenclature
198 are shown in Fig 1B. Indeed, both 5p and 3p arms of miR-616 have been shown to be
199 expressed in human cancers (11, 31). Next we evaluated the expression of miR-616-5p and
200 miR-616-3p in human cancers. Initially expression of miR-616-5p and miR-616-3p was
201 determined in various human cancer cell lines by qRT-PCR. We observed that endogenous
202 expression of miR-616-5p was higher than miR-616-3p in all the cell lines tested (**Fig 1C**). Next
203 we analysed the expression of miR-616-5p and miR-616-3p in the TCGA dataset from different
204 human cancers using OncomiR (http://www.oncomir.org), a web-based tool for miRNA
205 expression analysis. We observed a higher expression of miR-616-5p as compared to miR-
206 616-3p in all the cancer types evaluated (**Fig 2**). Of note the ratio of miR-616-5p and miR-616-
207 3p expression varied considerably across the different tissue types. These results suggest that
208 both 5p and 3p arms of miR-616 are expressed where miR-616-5p accumulates at higher
209 levels than miR-616-3p but their ratio is controlled in tissue-specific manner.
210

211 **Fig 1. Basal expression of miR-616-5p and miR-616-3p in human cancer cell lines**. (A)
212 Schematic representation of the CHOP locus is shown. The exons are shown in blue and gray
213 line between them represents intron. The miR-616 is located in the first intron. The arrows
214 show the direction of transcription of the gene. The protein coding regions are shown in
215 dark blue and untranslated regions are shown in light blue. (B) The name, accession number
216 and sequence of miR-616-5p and 3p are shown. (C) Total RNA from indicated cells was used
217 to determine the expression of miR-616-5p and miR-616-3p by qRT-PCR and normalised
218 against RNU6. Expression of miR-616-3p in MCF7 cells was arbitrarily set at 1. Error bars
219 represent mean ±S.D. from three independent experiments performed in triplicate. *P <
220 0.05, two-tailed unpaired t-test compared to miR-616-3p in MCF7 cells.
221
222 **Fig 2. Expression of miR-616-5p and miR-616-3p in human cancers**. Web-based algorithm
223 at (http://www.oncomir.org/) was used to assess the expression of miR-616-5p and miR-
224 616-3p. Log2 mean expression of miR-616-5p and 3p in indicated cancer types is shown. (N
225 = number samples in each cancer type). ACC: adrenocortical carcinoma; BLCA: bladder
226 urothelial carcinoma; BRCA: breast invasive carcinoma; CESC: cervical squamous cell
227 carcinoma and endocervical adenocarcinoma; CHOL: cholangiocarcinoma; COAD: colon

228 adenocarcinoma; ESCA: esophageal carcinoma; HNSC: head and neck squamous cell
229 carcinoma; KICH: kidney chromophobe; KIRC: kidney renal clear cell carcinoma; KIRP: kidney
230 renal papillary cell carcinoma; LGG: brain lower grade glioma; LIHC: liver hepatocellular
231 carcinoma; LUAD: lung adenocarcinoma; LUSC: lung squamous cell carcinoma; MESO:
232 mesothelioma; OV: ovarian serous cystadenocarcinoma; PAAD: pancreatic
233 adenocarcinoma; PCPG: pheochromocytoma and paraganglioma; PRAD: prostate
234 adenocarcinoma; READ: rectal adenocarcinoma; SARC: sarcoma; SKCM: skin cutaneous
235 melanoma; STAD: stomach adenocarcinoma; TGCT: testicular germ cell tumours; THCA:
236 thyroid carcinoma; THYM: thymoma; UCEC: uterine corpus endometrial carcinoma; UCS:
237 uterine carcinosarcoma; UVM: uveal melanoma
238
239

240 **Increased expression of miR-616-5p and miR-616-3p during UPR**

241 It was initially proposed that intronic miRNAs are derived from the same primary transcript
242 as their host genes thereby leading to co-expression and co-regulation of miRNA and cognate
243 host gene (27). Analysis of expression of 175 miRNAs and their host genes across twenty four
244 different human organs reported a significantly correlated expression profile (32). Recent
245 evidence however, shows significant discordant expression between intronic miRNAs and
246 host genes. Two likely explanations for this discordant expression are: (i) miRNAs have their
247 own independent promoters and (ii) crosstalk between microprocessor cleavage and mRNA
248 splicing (33, 34)**.** Next, we evaluated the co-regulation of miR-616 and its host gene (CHOP)
249 during conditions of UPR. MCF7, BT474 and HCT116 cells were either treated or untreated
250 with thapsigargin (TG) or Brefeldin A (BFA) for 24 hours and expression of CHOP, miR-616-5p
251 and miR-616-3p was determined. The expression level of CHOP, miR-616-5p and miR-616-3p
252 was upregulated in all three cell lines tested, during ER stress (**Fig. 3A-C**). Next we investigated
253 the role of ATF6, PERK and IRE1, three key mediators of the UPR in upregulation of miR-616
254 expression. For this purpose, we used MCF7 control (MCF7 PLKO) and knockdown of UPR
255 sensors (MCF7 XBP1-KD, MCF7 PERK-KD and MCF7 ATF6-KD) sub-clones of MCF7 (35). We
256 found that BFA-induced increase in the expression of CHOP, pri-miR-616, miR-616-5p and
257 miR-616-3p was attenuated in PERK-knockdown sub-clones of MCF7 (**Fig 4A**), whereas

258 knockdown of ATF6 or XBP1 had no significant effect (**Fig 4B-C**). These results suggest that
259 miR-616 is co-transcribed along with the CHOP transcript and attenuated PERK signalling
260 compromised the induction of both CHOP mRNA, pri-miR-616, miR-616-5p and miR-616-3p
261 during UPR.
262

263 **Fig 3. Upregulation of miR-616 (5p and 3p) and its host gene CHOP during UPR.** (A) MCF7
264 cells, (B) BT474 cells and (C) HCT116 cells were treated with (1 µM) TG or (0.5 µg/ml) BFA
265 for 24 hours. Expression of CHOP was quantified by RT-qPCR, normalized using RPLP0. The
266 expression level of miR-616 -5p and -3p was quantified by RT-qPCR, normalized using U6
267 snRNA. Error bars represent mean ±S.D. from three independent experiments performed in
268 triplicate. *P < 0.05, two-tailed unpaired t-test as compared to untreated control.
269

270 **Fig 4. Upregulation of miR-616 during ER stress is dependent on PERK pathway.** (A-C)
271 MCF7 PLKO, MCF7 XBP1-KD, MCF7 PERK-KD and MCF7 ATF6-KD sub-clones were treated
272 with (0.5 µg/ml) BFA for 24 hours. Expression level of CHOP and pri-miR-616 was quantified
273 by RT-qPCR, normalizing against RPLP0. The expression level of miR-616 -5p and -3p was
274 quantified by RT-qPCR, normalized using U6 snRNA. *P<0.05, **P < 0.001, two-tailed
275 unpaired t-test. N.S not significant.
276

277 MiR-616 targets c-MYC and reduces cell proliferation of breast cancer cells

278 Ye et al. reported that ectopic expression of miR-616-3p inhibited growth of MDA-MB231
279 cells while Arabkari did not find any effect of miR-616 overexpression in MDA-MB231 cells
280 (18) (25). Further, Yuan reported that miR-616-3p promoted growth and migration of MCF7
281 cells in contrast to Arabkari, who reported a decrease in growth and migration of miR-616
282 expressing MCF7 cells (19) (25). This could be due to different approaches used for
283 overexpression of miRNAs. Next, we used gain-of-function (overexpression) and loss-of-
284 function (CRISPR-Cas9 KO) approaches in MCF7 cells to study the role of miR-616 in breast
285 cancer. To better mimic the *in vivo* scenario we decided to use a lentiviral system for
286 modulating the expression of both miR-616-5p and -3p concurrently. For this purpose, MCF7
287 cells were transduced with lentivirus expressing GFP along with miR-616 or Cas-9 along with

288 gRNAs targeting miR-616. The expression of pri-miR-616, miR-616-5p and miR-616-3p was
289 determined in miR-616-overexpressing (MCF7-miR-616-OE) and miR-616-knockout (MCF7-
290 miR-616-KO) sub-clones of MCF7. As expected, the levels of pri-miR-616, miR-616-5p and
291 miR-616-3p were increased in MCF7-miR-616-OE sub-clone (**Fig. 5A**) and decreased in MCF7-
292 miR-616-KO sub-clone (**Fig. 5E**). The MCF7-miR-616-KO sub-clone displayed hypomorphic
293 phenotype with partial reduction in expression of pri-miR-616, miR-616-5p and miR-616-3p.
294 The miR-616 overexpressing (MCF7-miR-616-OE) sub-clone showed significantly decreased
295 cell growth (**Fig. 5B**), while the miR-616 knockout (MCF7-miR-616-KO) sub-clone showed
296 increased cell growth (**Fig. 5F**). This observation was further validated by colony formation
297 assay. The miR-616 overexpressing (MCF7-miR-616-OE) sub-clone of MCF7 cells showed
298 decrease in the number and size of the colonies (**Fig. 5C-D**) but miR-616 knockout (MCF7-miR-
299 616-KO) sub-clone showed an increase in the number and size of the colonies (**Fig. 5G-H**). We
300 found that expression of c-MYC mRNA and protein was reduced miR-616 overexpressing
301 (MCF7-miR-616-OE) sub-clone of MCF7 cells (**Fig. 6 A and C**) and increased in miR-616
302 knockout (MCF7-miR-616-KO) sub-clone (**Fig. 6 B and C**). Our results are in agreement with
303 an earlier report where ectopic expression of miR-616 was shown to inhibit growth of MCF7
304 cells accompanied by reduced expression of c-MYC (25). Since an inverse relationship
305 between the levels of expression of a miRNA and its target is anticipated, we evaluated
306 expression of c-MYC during conditions of UPR. We found the expression of c-MYC was
307 decreased in MCF7 (**Fig. 7A)** and BT474 (**Fig. 7B**) cells treated either with TG or BFA.
308 Furthermore, expression of c-MYC protein was decreased in MCF7 and BT474 cells upon
309 treatment with BFA (**Fig. 7C**). These results suggest a role for miR-616 in regulation of c-MYC
310 expression during conditions of UPR.

311 **Fig 5. MiR-616 reduces the proliferation of MCF7 cells.** (A) The expression of miR-616-3p,
312 miR-616-5p and pri-miR-616 is shown in MCF7-miR-CTRL and MCF7-miR-616-OE sub-clones
313 of MCF7. (B) MCF7-miR-CTRL and MCF7-miR-616-OE cells were plated and cell growth was
314 determined by x-CELLigence. (C-D) MCF7-miR-CTRL and MCF7-miR-616-OE cells were plated
315 in 6- well plate (1000 cells/well) and grown for 14 days. (C) Colonies stained with crystal
316 violet are shown. (D) Quantification of number of colonies for MCF7-miR-CTRL and MCF7-
317 miR-616-OE cells is shown. (E) The expression of miR-616-3p, miR-616-5p and pri-miR-616 is
318 shown in MCF7-Cas9-CTRL and MCF7-miR-616-KO sub-clones of MCF7. (F) MCF7-Cas9-CTRL
319 and MCF7-miR-616-KO cells were plated and cell growth was determined by x-CELLigence.
320 (G-H) MCF7-Cas9-CTRL and MCF7-miR-616-KO cells were plated in 6-well plate (1000
321 cells/well) and grown for 14 days. (G) Colonies stained with crystal violet are shown. (H)
322 Quantification of number of colonies for MCF7-Cas9-CTRL and MCF7-miR-616-KO cells is
323 shown.
324
325
326 **Fig 6. MiR-616 regulates the expression of c-MYC.** (A-B) Expression level of c-MYC mRNA is
327 shown in miR-616 knockout and miR-616 overexpressing sub-clones of MCF7 cells as
328 determined by qRT-PCR. Error bars represent mean ± S.D. from two independent
329 experiments performed in triplicate. *P < 0.05, two-tailed unpaired t-test as compared to
330 control. (C) The expression level of c-MYC protein is shown in miR-616 knockout and miR-
331 616 overexpressing sub-clones of MCF7 cells.
332
333 **Fig 7. Downregulation of c-MYC during UPR in breast cancer cells.** (A) MCF7 cells and (B)
334 BT474 cells were treated with (1 µM) TG or (0.5 µg/ml) BFA for 24 hours. Expression of c-
335 MYC was quantified by RT-qPCR, and normalized using RPLP0. Error bars represent mean
336 ±S.D. from three independent experiments performed in triplicate. (C) MCF7 BT474 cells
337 were treated with (0.5 µg/ml) BFA for indicated time points. Western blotting of total
338 protein was performed using antibodies for c-MYC and actin. Representative Immunoblot
339 and quantification of c-MYC expression normalised to actin are shown (n=3). *P < 0.05, two-
340 tailed unpaired t-test as compared to the untreated control.
341

342 ## MiR-616 modulates the expression of c-MYC via site in the ORF

343 To determine the mechanism of c-MYC regulation by miR-616, we used several bioinformatics
344 tools to search for the potential miR-616 binding sites in the reference sequence of c-MYC.
345 TargetScan (36) did not identify miR-616 binding sites in c-MYC. Interestingly, RNAhybrid
346 identified non-canonical miR-616-5p binding sites (at position 77, 2501 and 3076 bp) and miR-
347 616-3p binding sites (at position 614, 917 and 1525 bp) of c-MYC reference Sequence
348 (NM_002467.6) (**S1 Fig**). Furthermore, (miRWALK and RNAhybrid) picked an identical, non-

349 canonical miR-616-3p binding site in the protein-coding region (364-1728 bp) of c-MYC at
350 position 1525 bp (**Fig. 8A-B**). To test whether miR-616 down-regulates c-MYC via this site in
351 coding region, we co-transfected 293T cells with an expression vector containing the ORF of
352 c-MYC and miR-616 plasmid. Cell lysates were collected after 24 h and analysed by
353 immunoblotting. Our results showed that c-MYC protein level was strongly down-regulated
354 by co-expression of miR-616 (**Fig. 8C**). Under similar conditions, co-expression of miR-616 had
355 no effect on protein level of ERα (protein coding region of ERα has no predicted binding sites
356 for miR-616) (**Fig. 8D**). Further, co-expression of miR-4726 (miRNA that lacks binding sites in
357 the protein coding region of c-MYC) and c-MYC had no effect on c-MYC protein level (**Fig. 8E**).
358 Taken together these results suggest that miR-616 regulates the expression of c-MYC most
359 likely via the miR-616 response elements present in its protein coding region.
360

361 Fig 8. **Identification of a miR-616-3p-binding sites in the ORF of c-MYC.** Binding site for
362 miR-616-3p identified by (A) miRWALK and (B) RNAhybrid in protein coding region of c-MYC
363 reference sequence is shown. The secondary structure of miRNA-mRNA duplex is shown
364 with miR-616-3p in green and c-MYC mRNA in red. mfe: minimum free energy. (C) 293T cells
365 were transfected with plasmid containing c-MYC ORF in absence and presence of miR-616
366 plasmid. (D) 293T cells were transfected with plasmid containing ERα ORF in absence and
367 presence of miR-616 plasmid. (E) 293T cells were transfected with plasmid containing c-MYC
368 ORF in absence and presence of miR-4726 plasmid. Western blotting of total protein was
369 performed using the indicated antibodies. 24 h post-transfection western blotting of total
370 protein was performed using the indicated antibodies.
371

372 Prognostic value of the miR-616 in human cancers

373 We assessed the prognostic value of miR-616 in different cancer types using KM plotter. We
374 found that expression of miR-616 was associated with longer overall survival (OS) in cervical
375 squamous cell carcinoma, Head-neck squamous cell carcinoma, uterine corpus endometrial
376 carcinoma and Thymoma (**S2 Fig**). Surprisingly, the increased expression of miR-616 was
377 associated with shorter OS in esophageal adenocarcinoma, sarcoma, renal clear cell

carcinoma, lung squamous cell carcinoma and hepatocellular carcinoma (**S2 Fig**). Next, we used TNMplot to determine the expression of CHOP and miR-616 in normal and tumour tissue samples of breast. We found that expression of CHOP and miR-616 was reduced in tumour samples as compared to tumour adjacent normal tissue (**Fig 9A-B**). Further, the expression of miR-616 was associated with poor OS in luminal A subtype and better OS HER2 subtype of breast cancer (**Fig 9C**).

Fig 9. Prognostic value of miR-616 in subtypes of breast cancer. TNMplot (https://tnmplot.com/analysis/) was used to determine the expression of CHOP and miR-616 in human breast cancer. (A) Box plot for expression of CHOP in tumour (n=1097) and normal (n=403) tissues for human breast cancers is shown. (B) Box plot for expression of miR-616 in paired tumour (n=112) and tumour adjacent normal (n=112) for human breast cancers is shown. (C) KM Plotter (https://kmplot.com/) was used to determine the association of miR-616 with overall survival (OS) in subtypes of breast cancer.

DISCUSSION

MiRNAs regulate the wide range of cellular processes because of their ability to alter post-transcriptional gene expression (37). We have evaluated the role of UPR regulated miRNA-616 in cell growth and proliferation. We have shown that expression of miR-616 and its host gene (CHOP) is upregulated during ER stress in a PERK-dependent fashion (**Fig 4**). ER stress and UPR activation contributes to the initiation and progression of human diseases, such as cancer, neurodegenerative and cardiovascular disease (2, 38). We observed concordant expression of the CHOP and the mature miR-616 which suggests their transcriptional co-regulation (**Fig 3, 4**). Our results suggest a mechanism for increased expression of miR-616 in patho-physiological conditions where role of UPR is implicated.

Several studies have reported that miR-616 acts as a tumour promoting miRNA in human cancers (11, 31, 39). However, our results show that miR-616 expression attenuates the

405 proliferation of MCF7 cells while reduced expression of miR-616 increases it (**Fig 5**).
406 Furthermore, we observed that expression of miR-616 was reduced in human breast
407 cancers as compared to tumour adjacent normal tissue (**Fig 9**). In agreement with our
408 results miR-616-3p has been shown to potentiate apoptosis in HUVECs (16), inhibit head
409 and neck squamous cell carcinoma progression (17) and inhibit cell growth and
410 mammosphere formation of breast cancer cells (18, 25). Any small RNA having G-rich 6mer
411 seed sequence (nt 2-7 of the guide strand) can reduce viability of cells when associated with
412 RNA-induced silencing complex. G-rich seed sequence mediates toxicity by targeting C-rich
413 seed matches in the 3' UTR of genes critical for cell survival referred to as Death Induced by
414 Survival gene Elimination (DISE) (30). A systematic study to evaluate DISE activity of all 4096
415 possible 6mer seed sequences in six cell lines (three human and three mouse) revealed the
416 mechanism underlying this toxicity and a web-based algorithm (https://6merdb.org) can
417 predict the activity of an RNA with a known 6mer seed (40). Analysis of seed sequences
418 from both 5p and 3p strands of miR-616 revealed that both strands can exhibit opposing
419 effects on viability in a cell-type dependent manner (**S3 Fig**). Interestingly, several miRNAs
420 belonging to miR-371-373 Cluster (hsa-miR-371a-5p, hsa-miR-371b-5p, hsa-miR-372-5p and
421 hsa-miR-373-5p) that share seed sequence with miR-616-5p, have been shown to reduce
422 the progression and metastasis of colon cancer (41) as well as induction of cell cycle arrest
423 (42). Taken together, these observations indicate the presence of context-dependent
424 oncogenic and tumour suppressive effects of miR-616 in human cancers. Indeed context-
425 dependent tumour-promoting and tumour-suppressive role has been documented for
426 several miRNAs such as miR-17-92 cluster (43, 44). This cluster maps to a region frequently
427 amplified in Burkitt's lymphoma, diffuse large B-cell lymphoma, follicular lymphoma and
428 lung cancer (26, 43). The expression of miR-17-92 is reduced in prostate cancer (17) and

429 miR-17-92 expression in intestinal epithelial cells inhibited colon cancer progression by
430 suppressing tumour angiogenesis (17).
431
432 Studies on target recognition by miRNAs have shown that sequence complementarity at the
433 5' end of the miRNA, the so-called "seed region" at positions 2 to 7, is a main determinant
434 for target recognition (36). However, a perfect seed match of its own is not a good predictor
435 for miRNA regulation and a number of studies have shown that miRNA can regulate the
436 expression of target genes via the sites with a G: U wobble and/or mismatch in the seed
437 region (36). Further, a study using a cross-linking and immunoprecipitation method to
438 experimentally identify microRNA target sites in an unbiased manner has reported a
439 significant number of non-canonical sites (45, 46). Hence, presence of perfect seed
440 complementarity is not essential for regulation of target genes by miRNA. In addition, target
441 sites for endogenous miRNAs have been reported in ORFs and 5’ UTRs, but they are less
442 frequent than those in the 3’ UTR (47, 48). We found a non-canonical miR-616-3p binding
443 site in the protein coding region of c-MYC transcript (**Fig 8**). Several studies have reported
444 the presence of miRNA-binding sites in the protein coding sequence of the genes. Indeed
445 miRNAs have been shown to regulate embryonic stem cell differentiation, DNA methylation,
446 regulation of apoptosis, aortic development, and tumour suppression via the functional
447 miRNA-binding sites in the protein coding sequence of the target genes (47, 48, 49). Several
448 studies have reported the upregulation of c-MYC in different cancer cells and tumours such
449 as neuroblastomas, lung, and breast cancer (50). The expression of c-MYC was
450 downregulated in miR-616 expressing and upregulated in miR-616 knockout MCF7 cells (**Fig**
451 **6**). These observations suggest that effects of miR-616 on cell growth are primarily mediated
452 by downregulation of c-MYC.

453

454 PERK has been shown to act as a haploinsufficient tumour suppressor, where the nature of
455 its function is determined by gene dose (51, 52). Transient pause in protein synthesis due to
456 eIF2α phosphorylation by PERK is beneficial by reducing secretory load in the ER.
457 Phosphorylation of NRF2 by PERK attenuates Keap1-mediated degradation of NRF2 and
458 promotes expression of anti-oxidant enzymes through the antioxidant response elements
459 (53, 54). PERK signalling can upregulate the CHOP/DDIT3 transcription factor, which inhibits
460 expression of the gene encoding anti-apoptotic BCL-2 to hasten cell death, in addition to
461 enhancing the expression of pro-apoptotic BCL-2 members such as BIM (54). Studies in both
462 cellular and animal models with CHOP gene deficiency have shed light on the pro-apoptotic
463 role of CHOP during cellular stress (54). Further, ectopic expression of CHOP was reported to
464 induce a G1 cell cycle arrest (55). CHOP maintains the integrity of the human hematopoietic
465 stem cell (HSC) pool by eliminating HSCs harbouring oncogenic mutations, and decrease the
466 risk of leukaemia. CHOP induction triggers apoptosis of premalignant cells to prevent
467 malignant progression in a mouse lung cancer model. Hepatocyte-specific CHOP ablation
468 increased tumourigenesis in high fat diet-induced steatohepatitis and Hepatocellular
469 carcinoma (56, 57). CHOP has been shown to promote cancer progression, when fused with
470 FUS/TLS or EWS protein by genomic rearrangement (58, 59). The FUS-CHOP oncoprotein has
471 been shown to induce metastasis in in vivo model of sarcoma (58). Accumulating data suggest
472 that CHOP impinges upon several aspects of cancer including initiation as well as progression
473 of tumours (54). Our results show that miR-616 supressed cell growth of cancer cells through
474 suppressing c-MYC expression. Our results establish a new and unexpected role for the CHOP
475 locus by providing evidence that miR-616 can inhibit cell proliferation by targeting c-MYC.

476

ACKNOWLEDGEMENTS

We are grateful to the Technical Officers and administrative team in Pathology, School of Medicine at University of Galway, Ireland.

REFERENCES

1. Hetz C, Zhang K, Kaufman RJ. Mechanisms, regulation and functions of the unfolded protein response. Nat Rev Mol Cell Biol. 2020;21(8):421-38.
2. Hetz C, Axten JM, Patterson JB. Pharmacological targeting of the unfolded protein response for disease intervention. Nat Chem Biol. 2019;15(8):764-75.
3. Barua D, Gupta A, Gupta S. Targeting the IRE1-XBP1 axis to overcome endocrine resistance in breast cancer: Opportunities and challenges. Cancer Lett. 2020;486:29-37.
4. Nadanaka S, Okada T, Yoshida H, Mori K. Role of disulfide bridges formed in the luminal domain of ATF6 in sensing endoplasmic reticulum stress. Mol Cell Biol. 2007;27(3):1027-43.
5. Yoshida H, Okada T, Haze K, Yanagi H, Yura T, Negishi M, et al. ATF6 activated by proteolysis binds in the presence of NF-Y (CBF) directly to the cis-acting element responsible for the mammalian unfolded protein response. Mol Cell Biol. 2000;20(18):6755-67.
6. Cullinan SB, Zhang D, Hannink M, Arvisais E, Kaufman RJ, Diehl JA. Nrf2 is a direct PERK substrate and effector of PERK-dependent cell survival. Mol Cell Biol. 2003;23(20):7198-209.
7. Harding HP, Zhang Y, Bertolotti A, Zeng H, Ron D. Perk is essential for translational regulation and cell survival during the unfolded protein response. Mol Cell. 2000;5(5):897-904.
8. Ha M, Kim VN. Regulation of microRNA biogenesis. Nat Rev Mol Cell Biol. 2014;15(8):509-24.
9. Ma S, Chan YP, Kwan PS, Lee TK, Yan M, Tang KH, et al. MicroRNA-616 induces androgen-independent growth of prostate cancer cells by suppressing expression of tissue factor pathway inhibitor TFPI-2. Cancer Res. 2011;71(2):583-92.
10. Zhang S, Zhang X, Chen G, Zheng X, Zhu X, Shan L. Hsa_circ_0007494 suppresses prostate cancer progression via miR-616/PTEN axis. Exp Cell Res. 2020;395(2):112233.
11. Wu ZH, Lin C, Liu CC, Jiang WW, Huang MZ, Liu X, et al. MiR-616-3p promotes angiogenesis and EMT in gastric cancer via the PTEN/AKT/mTOR pathway. Biochem Biophys Res Commun. 2018;501(4):1068-73.
12. Wang DX, Zou YJ, Zhuang XB, Chen SX, Lin Y, Li WL, et al. Sulforaphane suppresses EMT and metastasis in human lung cancer through miR-616-5p-mediated GSK3β/β-catenin signaling pathways. Acta Pharmacol Sin. 2017;38(2):241-51.
13. Zhang D, Zhou P, Wang W, Wang X, Li J, Sun X, et al. MicroRNA-616 promotes the migration, invasion and epithelial-mesenchymal transition of HCC by targeting PTEN. Oncol Rep. 2016;35(1):366-74.
14. Bai QL, Hu CW, Wang XR, Shang JX, Yin GF. MiR-616 promotes proliferation and inhibits apoptosis in glioma cells by suppressing expression of SOX7 via the Wnt signaling pathway. Eur Rev Med Pharmacol Sci. 2017;21(24):5630-7.
15. Fan MQ, Huang CB, Gu Y, Xiao Y, Sheng JX, Zhong L. Decrease expression of microRNA-20a promotes cancer cell proliferation and predicts poor survival of hepatocellular carcinoma. J Exp Clin Cancer Res. 2013;32(1):21.
16. Chen H, Liu X, Wu Y, Wu X, Wen X, Lu Y, et al. Apoptosis in HUVECs induced by microRNA-616-3p via X-linked inhibitor of apoptosis protein targeting. Exp Ther Med. 2021;21(6):661.

520 17. Hou Y, Zhou M, Li Y, Tian T, Sun X, Chen M, et al. Risk SNP-mediated LINC01614 upregulation
521 drives head and neck squamous cell carcinoma progression via PI3K/AKT signaling pathway. Mol
522 Carcinog. 2022;61(8):797-811.
523 18. Ye G, Pan R, Zhu L, Zhou D. Circ_DCAF6 potentiates cell stemness and growth in breast
524 cancer through GLI1-Hedgehog pathway. Exp Mol Pathol. 2020;116:104492.
525 19. Yuan C. miR-616 promotes breast cancer migration and invasion by targeting TIMP2 and
526 regulating MMP signaling. Oncol Lett. 2019;18(3):2348-55.
527 20. Gupta A, Hossain MM, Read DE, Hetz C, Samali A, Gupta S. PERK regulated miR-424(322)-503
528 cluster fine-tunes activation of IRE1 and ATF6 during Unfolded Protein Response. Sci Rep.
529 2015;5:18304.
530 21. Gupta S, Read DE, Deepti A, Cawley K, Gupta A, Oommen D, et al. Perk-dependent
531 repression of miR-106b-25 cluster is required for ER stress-induced apoptosis. Cell Death Dis.
532 2012;3(6):e333.
533 22. Cawley K, Logue SE, Gorman AM, Zeng Q, Patterson J, Gupta S, et al. Disruption of microRNA
534 biogenesis confers resistance to ER stress-induced cell death upstream of the mitochondrion. PLoS
535 One. 2013;8(8):e73870.
536 23. Read DE, Gupta A, Ladilov Y, Samali A, Gupta S. miRNA signature of unfolded protein
537 response in H9c2 rat cardiomyoblasts. Cell Biosci. 2014;4(1):56.
538 24. Hiramatsu N, Chiang K, Aivati C, Rodvold JJ, Lee JM, Han J, et al. PERK-mediated induction of
539 microRNA-483 disrupts cellular ATP homeostasis during the unfolded protein response. J Biol Chem.
540 2020;295(1):237-49.
541 25. Arabkari V. *Regulation of cell fate by microRNAs during unfolded protein response*

542 *and its role in cancer* [Doctor of Philosophy]. Galway: National University of Ireland Galway, Ireland;
543 (2018) https://aran.library.nuigalway.ie/handle/10379/14750.
544 26. Hossain MM, Sultana A, Barua D, Islam MN, Gupta A, Gupta S. Differential expression,
545 function and prognostic value of miR-17-92 cluster in ER-positive and triple-negative breast cancer.
546 Cancer Treat Res Commun. 2020;25:100224.
547 27. Salim U, Kumar A, Kulshreshtha R, Vivekanandan P. Biogenesis, characterization, and
548 functions of mirtrons. Wiley Interdiscip Rev RNA. 2022;13(1):e1680.
549 28. Mitra R, Lin CC, Eischen CM, Bandyopadhyay S, Zhao Z. Concordant dysregulation of miR-5p
550 and miR-3p arms of the same precursor microRNA may be a mechanism in inducing cell proliferation
551 and tumorigenesis: a lung cancer study. RNA. 2015;21(6):1055-65.
552 29. Kozomara A, Griffiths-Jones S. miRBase: annotating high confidence microRNAs using deep
553 sequencing data. Nucleic Acids Res. 2014;42(Database issue):D68-73.
554 30. Putzbach W, Gao QQ, Patel M, Haluck-Kangas A, Murmann AE, Peter ME. DISE: A Seed-
555 Dependent RNAi Off-Target Effect That Kills Cancer Cells. Trends Cancer. 2018;4(1):10-9.
556 31. Ren W, Hu J, Li H, Chen J, Ding J, Zu X, et al. miR-616-5p Promotes Invasion and Migration of
557 Bladder Cancer. Front Oncol. 2021;11:762946.
558 32. Baskerville S, Bartel DP. Microarray profiling of microRNAs reveals frequent coexpression
559 with neighboring miRNAs and host genes. RNA. 2005;11(3):241-7.
560 33. Schanen BC, Li X. Transcriptional regulation of mammalian miRNA genes. Genomics.
561 2011;97(1):1-6.
562 34. Agranat-Tamir L, Shomron N, Sperling J, Sperling R. Interplay between pre-mRNA splicing
563 and microRNA biogenesis within the supraspliceosome. Nucleic Acids Res. 2014;42(7):4640-51.
564 35. Hossain MM, Barua D, Arabkari V, Islam N, Gupta A, Gupta S. Hyperactivation of nuclear
565 receptor coactivators induces PERK-dependent cell death. Oncotarget. 2018;9(14):11707-21.
566 36. Agarwal V, Bell GW, Nam JW, Bartel DP. Predicting effective microRNA target sites in
567 mammalian mRNAs. Elife. 2015;4.
568 37. Jin HY, Xiao C. MicroRNA Mechanisms of Action: What have We Learned from Mice? Front
569 Genet. 2015;6:328.

38. Doyle KM, Kennedy D, Gorman AM, Gupta S, Healy SJ, Samali A. Unfolded proteins and endoplasmic reticulum stress in neurodegenerative disorders. J Cell Mol Med. 2011;15(10):2025-39.
39. Zhou Y, Meng P, Tang B, Ke Z, Liu L, Chen Y, et al. MiR-616 promotes the progression of pancreatic carcinoma by targeting OXR1. Minerva Med. 2021;112(4):528-9.
40. Bartom ET, Kocherginsky M, Paudel B, Vaidyanathan A, Haluck-Kangas A, Patel M, et al. SPOROS: A pipeline to analyze DISE/6mer seed toxicity. PLoS Comput Biol. 2022;18(3):e1010022.
41. Ullmann P, Rodriguez F, Schmitz M, Meurer SK, Qureshi-Baig K, Felten P, et al. The miR-371~373 Cluster Represses Colon Cancer Initiation and Metastatic Colonization by Inhibiting the TGFBR2/ID1 Signaling Axis. Cancer Res. 2018;78(14):3793-808.
42. Langroudi L, Jamshidi-Adegani F, Shafiee A, Rad SM, Keramati F, Azadmanesh K, et al. MiR-371-373 cluster acts as a tumor-suppressor-miR and promotes cell cycle arrest in unrestricted somatic stem cells. Tumour Biol. 2015;36(10):7765-74.
43. Zhao W, Gupta A, Krawczyk J, Gupta S. The miR-17-92 cluster: Yin and Yang in human cancers. Cancer Treat Res Commun. 2022;33:100647.
44. Yu L, Ma W, Song B, Wang S, Li X, Wang Z. Hsa_circ_0030042 Ameliorates Oxidized Low-Density Lipoprotein-Induced Endothelial Cell Injury via the MiR-616-3p/RFX7 Axis. Int Heart J. 2022;63(4):763-72.
45. Stavast CJ, Erkeland SJ. The Non-Canonical Aspects of MicroRNAs: Many Roads to Gene Regulation. Cells. 2019;8(11).
46. Dai W, Su X, Zhang B, Wu K, Zhao P, Yan Z. An Alternative Class of Targets for microRNAs Containing CG Dinucleotide. Biology (Basel). 2022;11(3).
47. Qin W, Shi Y, Zhao B, Yao C, Jin L, Ma J, et al. miR-24 regulates apoptosis by targeting the open reading frame (ORF) region of FAF1 in cancer cells. PLoS One. 2010;5(2):e9429.
48. Duursma AM, Kedde M, Schrier M, le Sage C, Agami R. miR-148 targets human DNMT3b protein coding region. RNA. 2008;14(5):872-7.
49. Tay Y, Zhang J, Thomson AM, Lim B, Rigoutsos I. MicroRNAs to Nanog, Oct4 and Sox2 coding regions modulate embryonic stem cell differentiation. Nature. 2008;455(7216):1124-8.
50. Dang CV. MYC on the path to cancer. Cell. 2012;149(1):22-35.
51. Pytel D, Gao Y, Mackiewicz K, Katlinskaya YV, Staschke KA, Paredes MC, et al. PERK Is a Haploinsufficient Tumor Suppressor: Gene Dose Determines Tumor-Suppressive Versus Tumor Promoting Properties of PERK in Melanoma. PLoS Genet. 2016;12(12):e1006518.
52. Gupta S, Giricz Z, Natoni A, Donnelly N, Deegan S, Szegezdi E, et al. NOXA contributes to the sensitivity of PERK-deficient cells to ER stress. FEBS Lett. 2012;586(22):4023-30.
53. Pytel D, Majsterek I, Diehl JA. Tumor progression and the different faces of the PERK kinase. Oncogene. 2016;35(10):1207-15.
54. Oyadomari S, Mori M. Roles of CHOP/GADD153 in endoplasmic reticulum stress. Cell Death Differ. 2004;11(4):381-9.
55. Jauhiainen A, Thomsen C, Strombom L, Grundevik P, Andersson C, Danielsson A, et al. Distinct cytoplasmic and nuclear functions of the stress induced protein DDIT3/CHOP/GADD153. PLoS One. 2012;7(4):e33208.
56. Toriguchi K, Hatano E, Tanabe K, Takemoto K, Nakamura K, Koyama Y, et al. Attenuation of steatohepatitis, fibrosis, and carcinogenesis in mice fed a methionine-choline deficient diet by CCAAT/enhancer-binding protein homologous protein deficiency. J Gastroenterol Hepatol. 2014;29(5):1109-18.
57. Rahman SM, Schroeder-Gloeckler JM, Janssen RC, Jiang H, Qadri I, Maclean KN, et al. CCAAT/enhancing binding protein beta deletion in mice attenuates inflammation, endoplasmic reticulum stress, and lipid accumulation in diet-induced nonalcoholic steatohepatitis. Hepatology. 2007;45(5):1108-17.
58. Pérez-Losada J, Pintado B, Gutiérrez-Adán A, Flores T, Bañares-González B, del Campo JC, et al. The chimeric FUS/TLS-CHOP fusion protein specifically induces liposarcomas in transgenic mice. Oncogene. 2000;19(20):2413-22.

621 59. Matsui Y, Ueda T, Kubo T, Hasegawa T, Tomita Y, Okamoto M, et al. A novel type of EWS-
622 CHOP fusion gene in myxoid liposarcoma. Biochem Biophys Res Commun. 2006;348(2):437-40.

623

624 Supporting information

625 S1 Fig. **Identification of a miR-616-5p and miR-616-3p -binding sites in the c-Myc.**
626 RNAhybrid analysis of c-MYC reference sequence and miR-616. The secondary structure of
627 miRNA-mRNA duplex is shown with miRNA in green and mRNA in red. mfe: minimum free
628 energy.

629

630 S2 Fig. **Association between miR-616 expression and overall survival in human cancer**.
631 Web-based algorithm KM plotter (http://kmplot.com/analysis/) was used to evaluate the
632 association between miR-616 with overall (OS) survival.

633

634 S3 Fig. **Prediction of the effect of miR-616-5p and miR-616-3p on cell viability through their**
635 **6mer seed sequence.** The activity of 6-mer seed of was evaluated in three human (HeyA8-
636 ovarian, H460-lung and H4-brain) and three mouse (M565-liver, 3LL-lung and GL261-brain)
637 cell lines. MiRNAs with low viability (high toxicity) are shown in red and with high viability
638 (low toxicity) are shown in green. Predominantly expressed mature miRNAs (guide miRNA)
639 are shown in dark purple while lesser expressed (passenger miRNA) are shown in light
640 purple. The miRNAs sharing seed sequence with miR-616-5p are also shown.

A

B

CHOP (NM_001195053.1)

miRNA	Other name	Accession number	Sequence 5' to 3'
hsa-miR-616-5p	hsa-miR-616*	MIMAT0003284	ACUCAAAACCCUUCAGUGACUU
hsa-miR-616-3p	hsa-miR-616	MIMAT0004805	AGUCAUUGGAGGGUUUGAGCAG

C

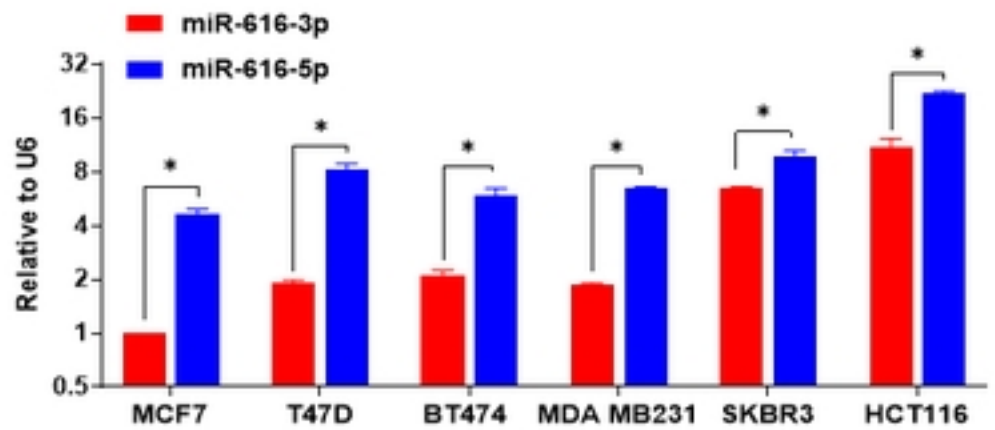

Figure 1

Figure 1

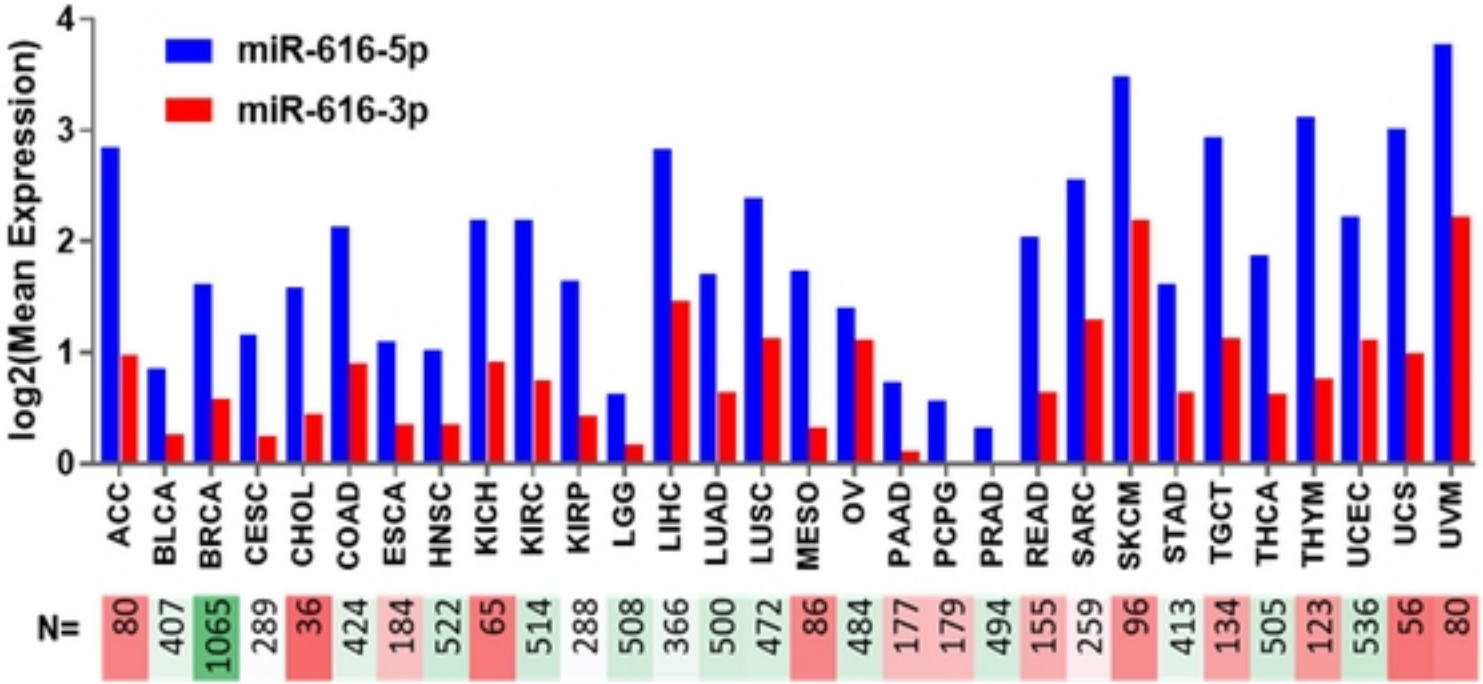

Figure 2

Figure 2

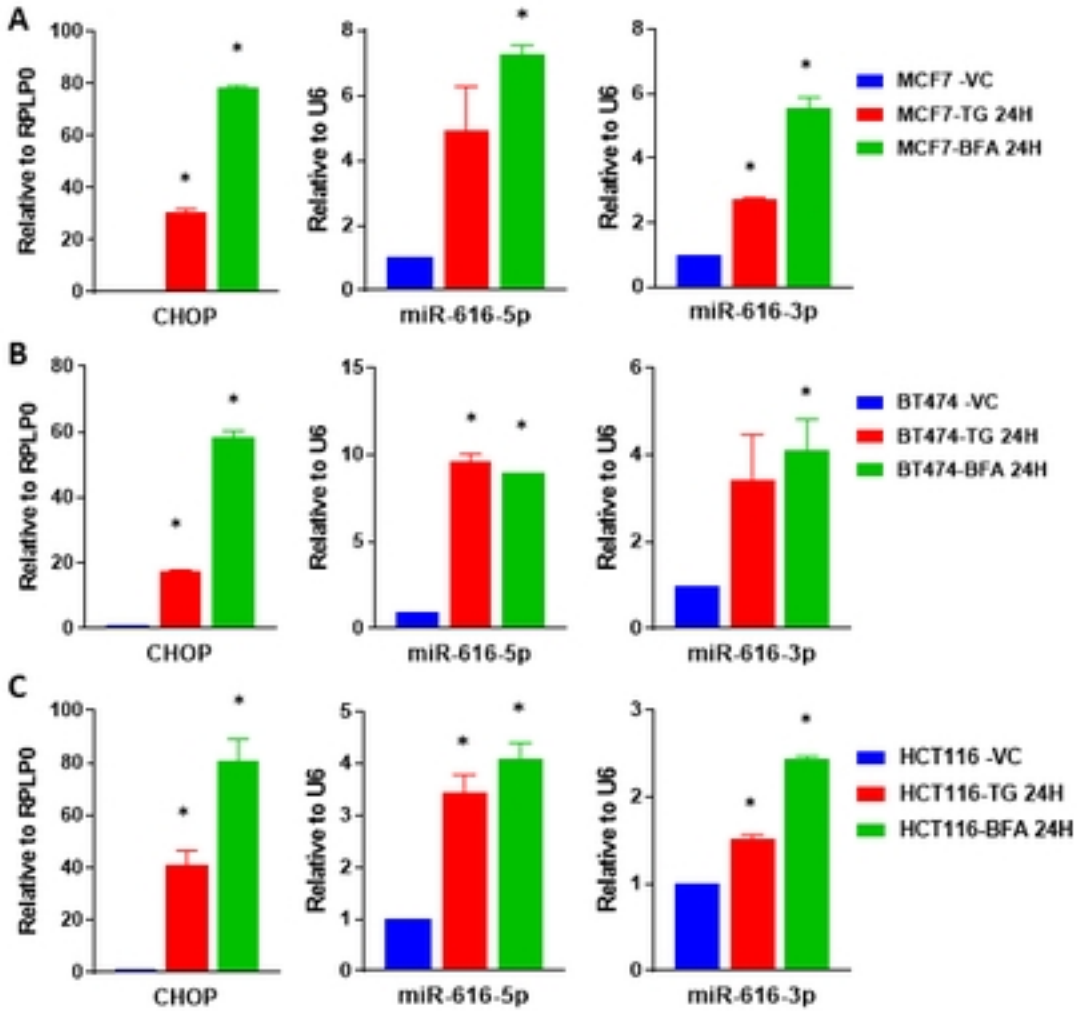

Figure 3

Figure 3

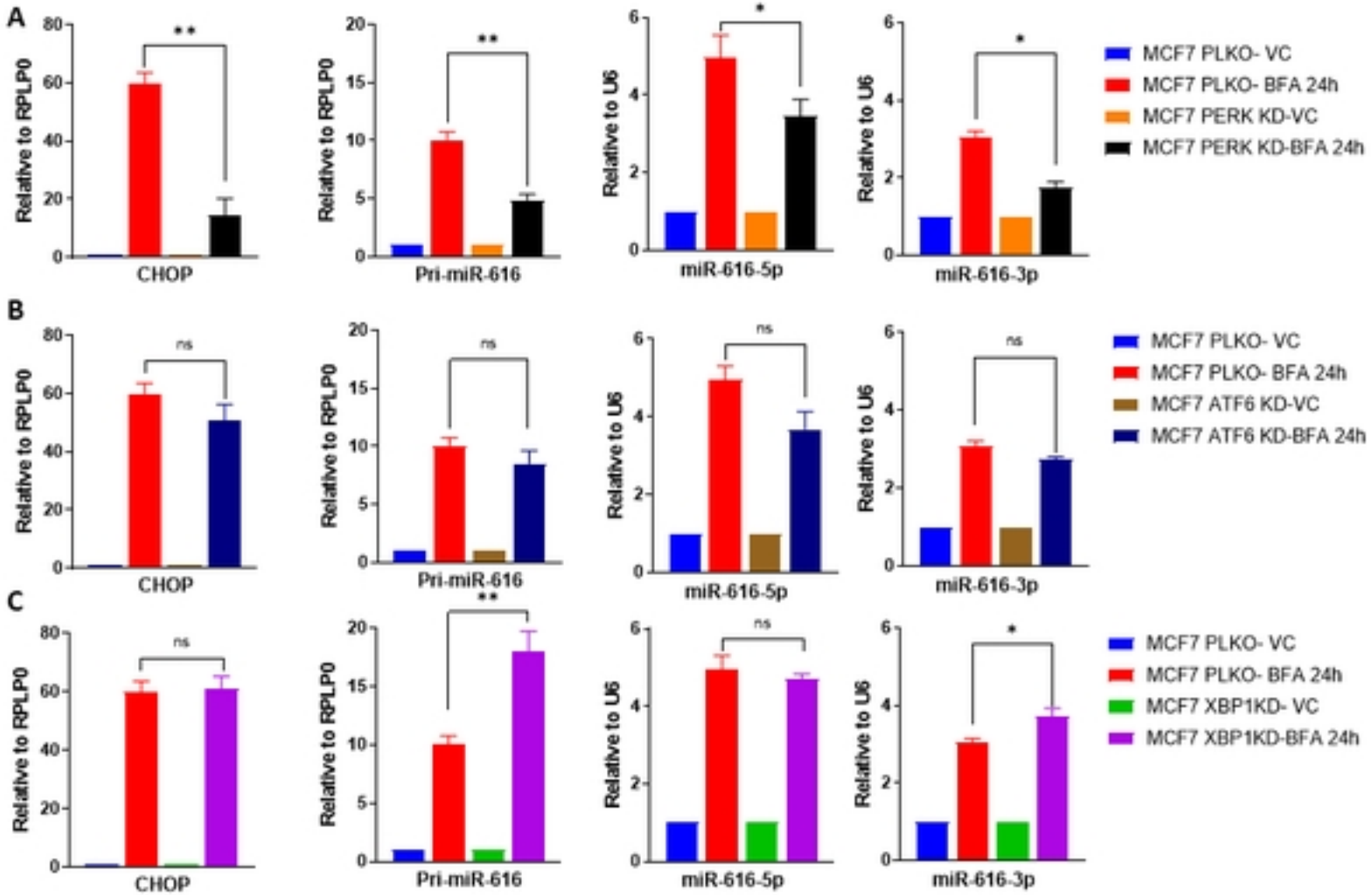

Figure 4

Figure 4

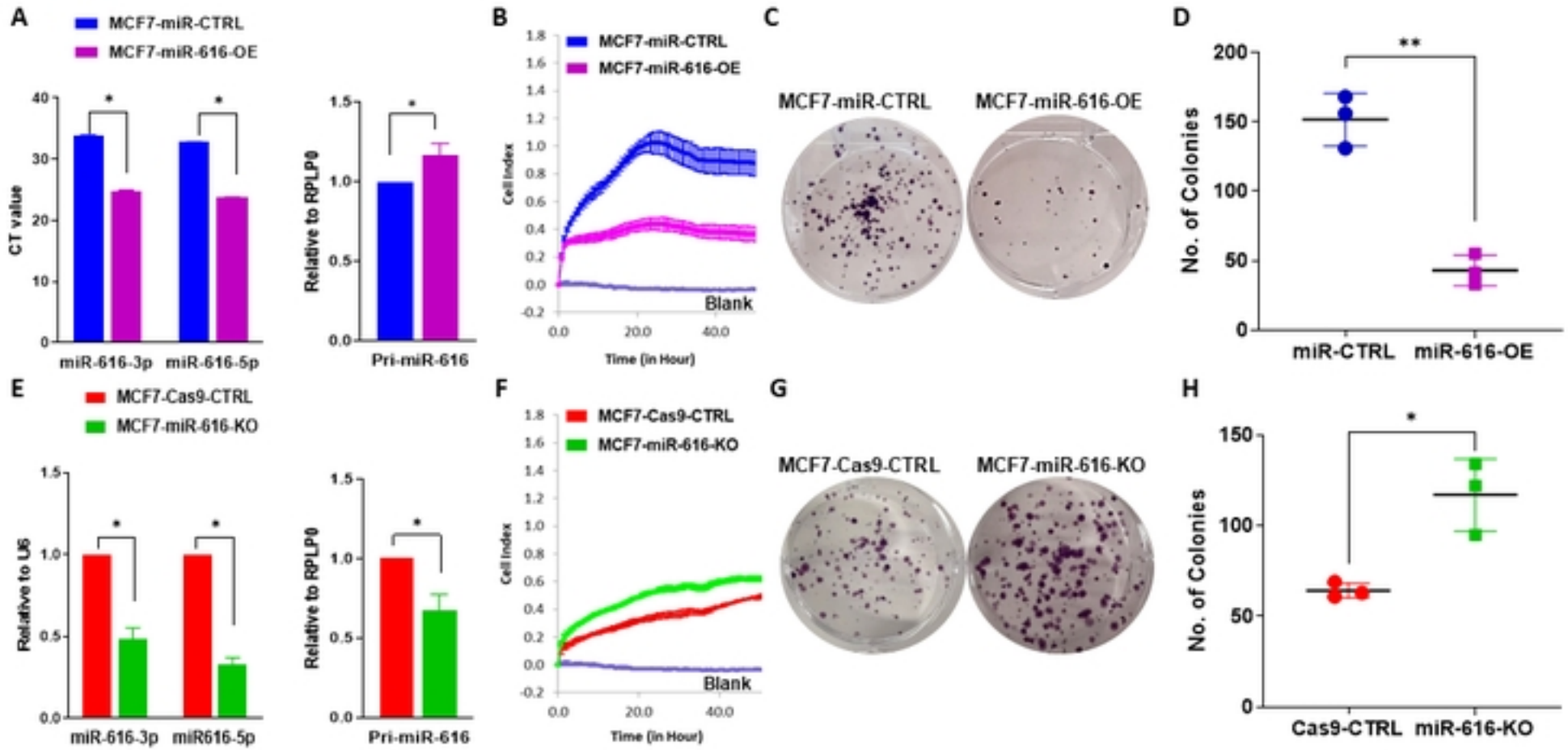

Figure 5

Figure 5

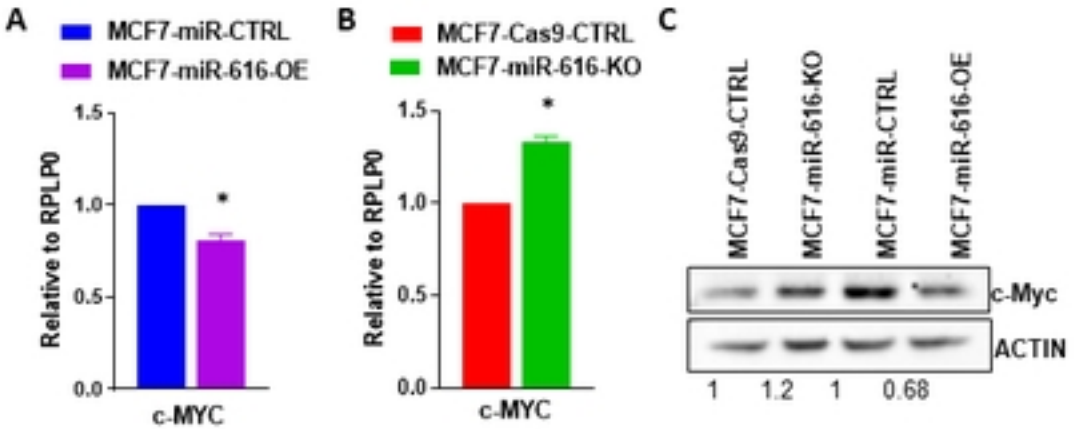

Figure 6

Figure 6

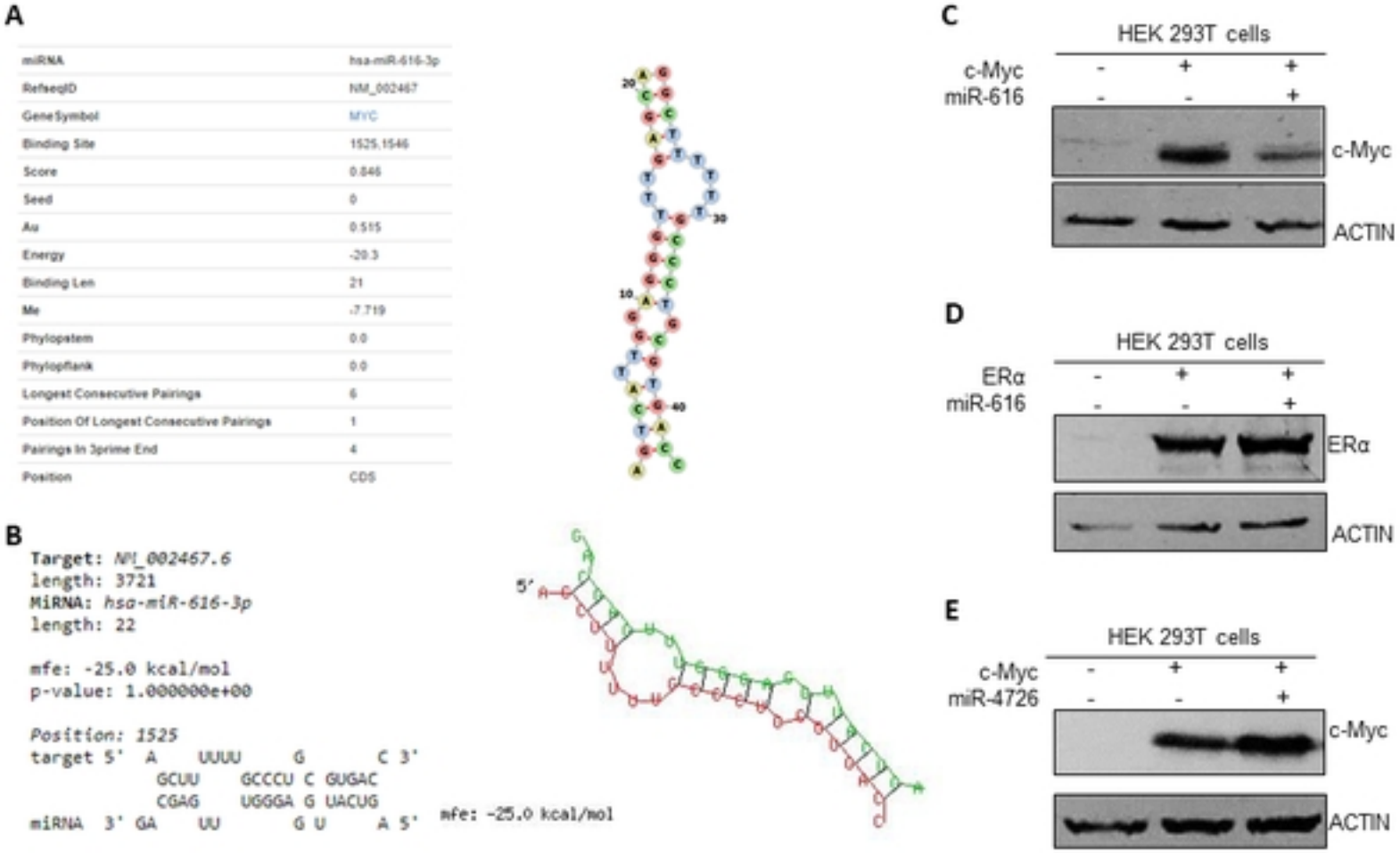

Figure 8

Figure 8

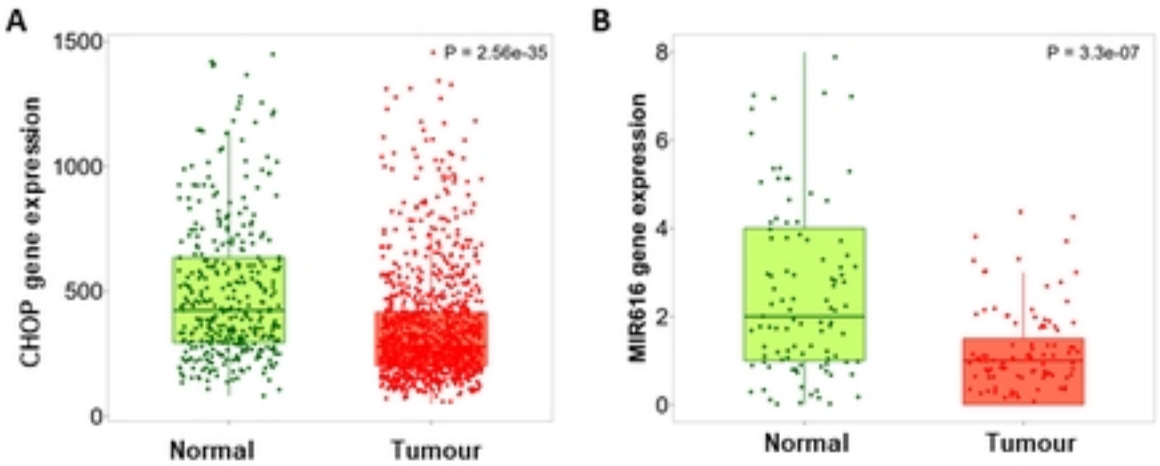

C

Subtypes of breast cancer	Overall survival	
	Hazard Ratio	Logrank P
Luminal A	1.57 (1.08 - 2.27)	**0.01600**
Luminal B	0.81 (0.60 - 1.11)	0.19000
HER2	0.31 (0.16 - 0.61)	**0.00034**
TNBC	0.75 (0.46 - 1.21)	0.24000

Figure 9

Figure 9

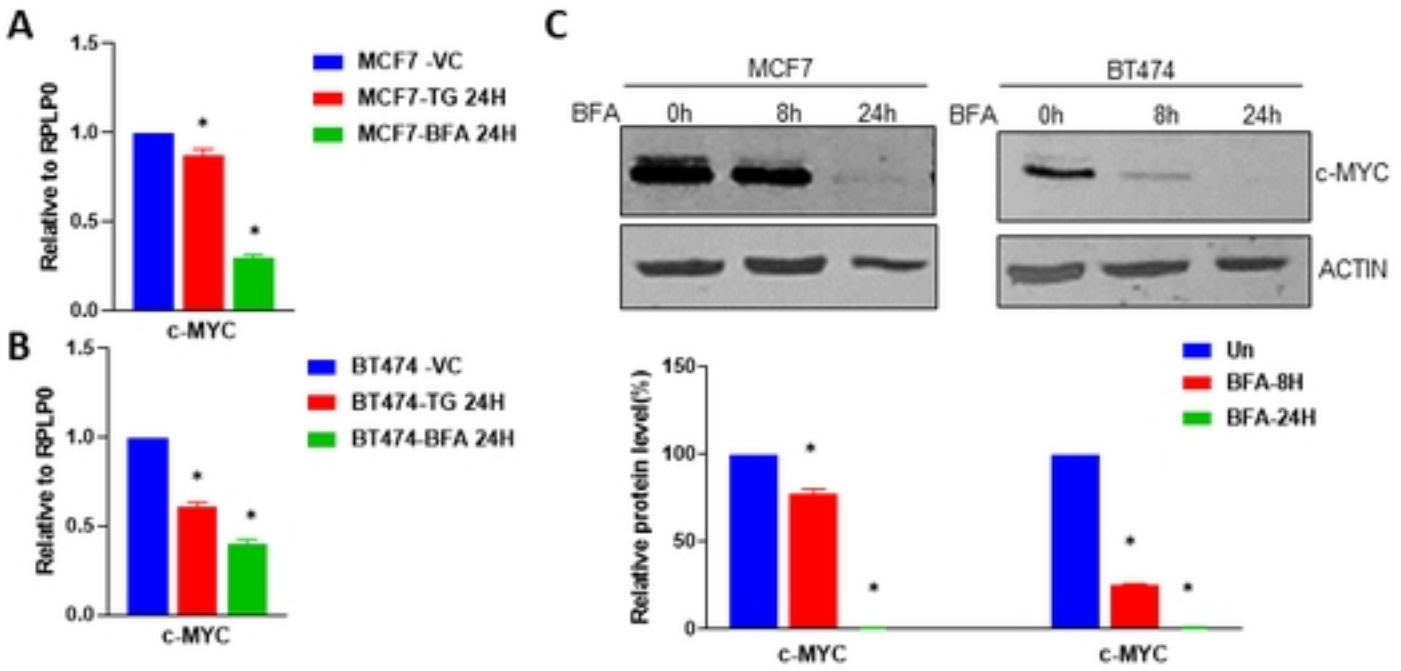

Figure 7

Figure 7